Cephalopod Biodiversity, Ecology and Evolution
Payne, A. I. L., Lipiński, M. R., Clarke, M. R. and M. A. C. Roeleveld (Eds). *S. Afr. J. mar. Sci. 20: 255–265*

ILLEX ARGENTINUS DERIVED FROM ARTIFICIAL FERTILIZATION

M. SAKAI, N. E. BRUNETTI†, B. ELENA† and Y. SAKURAI‡*

The embryonic and early post-hatching development of artificially fertilized eggs of *Illex argentinus* was observed at several temperatures from 8.5 to 23.2°C. During the fertilization procedure, oviducal gland jelly was added to eggs (about 1.0 mm long). Chorion expansion began 20 minutes after fertilization and continued throughout embryonic development. Before hatching, the chorion diameter measured more than 2.5 mm. Developmental stages were described on the basis of morphological features. Most hatchlings from the least disturbed eggs had well-developed ink sacs, fins, extensible probosces and buccal masses. The mantle length of hatchlings was approximately 1.6 mm. Comparisons are made with embryos and hatchlings of other ommastrephid squid, *Illex* species and *Todarodes pacificus*.

Stocks of the Argentine shortfin squid *Illex argentinus* support the most commercially important cephalopod fishery in the South-West Atlantic. Knowledge of the reproductive biology and early life history of the species is limited, however, because studies on its life cycle are largely dependent on fisheries data or restricted information from research cruises (Rodhouse *et al*. 1995). Paralarval distribution patterns suggest that spawning takes place at temperatures >12°C on the continental shelf between 43 and 46°S during summer (Brunetti 1990), as well as in subtropical waters of the Brazil Current (Brunetti *et al*. 1991, Haimovici *et al*. 1995).

Until recently, observations on the embryonic and hatchling biology of ommastrephid squid depended on chance collections of natural egg masses (Naef 1921–1923) or on having captive females spawn egg masses in tanks (Hamabe 1961a, b, Boletzky *et al*. 1973, O'Dor *et al*. 1977, Bower and Sakurai 1996). However, embryos and paralarval hatchlings can be studied using artificial fertilization techniques, such as those developed for *Ommastrephes bartramii, Sthenoteuthis oualaniensis* (Sakurai *et al*. 1995) and *Todarodes pacificus* (Ikeda *et al*. 1993, Sakurai *et al*. 1996). Sakai and Brunetti (1997) also used this general technique successfully on *I. argentinus* eggs.

Naef (1921–1923) proposed developmental stages for ommastrephid (probably *Illex coindetii*) embryos using the criterion of age, and O'Dor *et al*. (1982) described embryonic development for *I. illecebrosus* according to Naef's (1921–1923) stages. However, those authors did not provide complete atlases. Watanabe *et al*. (1996) established the embryonic stages of *T. pacificus*, on the basis of the morphological features proposed for *Loligo* by Arnold (1965). In the present study, the developmental stages up to hatching of *I. argentinus* embryos obtained from artificially fertilized eggs are described and a complete atlas of 30 stages, based on morphological features, is presented. Features of the hatchling are also compared with those of other ommastrephid hatchlings. Finally, the statoliths are described.

MATERIAL AND METHODS

Live squid were caught with a bottom trawl during two cruises of the R.V. *Capitan Oca Balda* in two areas: over the south Patagonian shelf from 45 to 47°S in February 1997, and over the Bonaerensis shelf from 37 to 39°S in April 1997. Mature males and females were removed from the catch, placed in a fibreglass reinforced plastic circular tank of 1m^3 on board and transported to the laboratory. Artificial fertilization was performed either on board or in the laboratory. Sperm were obtained from females that had already copulated (Maturity Stage VI, according to Brunetti 1990), using spermatangia implanted at the bases of the gills, and spermatophores from mature males. The artificial fertilization technique used has already been described by Sakurai *et al*. (1995) and Sakai and Brunetti (1997).

Fertilized eggs were divided into groups of 100–200 and placed in petri dishes containing filtered, oxygenated seawater. The procedure of artificial fertilization, which required about 15 minutes per female, was conducted at room temperature (15–20°C). The

* JICA-INIDEP, CC-175, Mar del Plata, 7600 Argentina. Email: sakai@argenet.com.ar
† Instituto Nacional de Investigación y Desarrollo Pesquero (INIDEP), CC-175, Mar del Plata, 7600 Argentina. Email: calamar@inidep.edu.ar
‡ Faculty of Fisheries, Hokkaido University, 3-1-1 Minato-cho, Hakodate, Hokkaido 041, Japan. Email: sakurai@pop.fish.hokudai.ac.jp

Manuscript received: September 1997

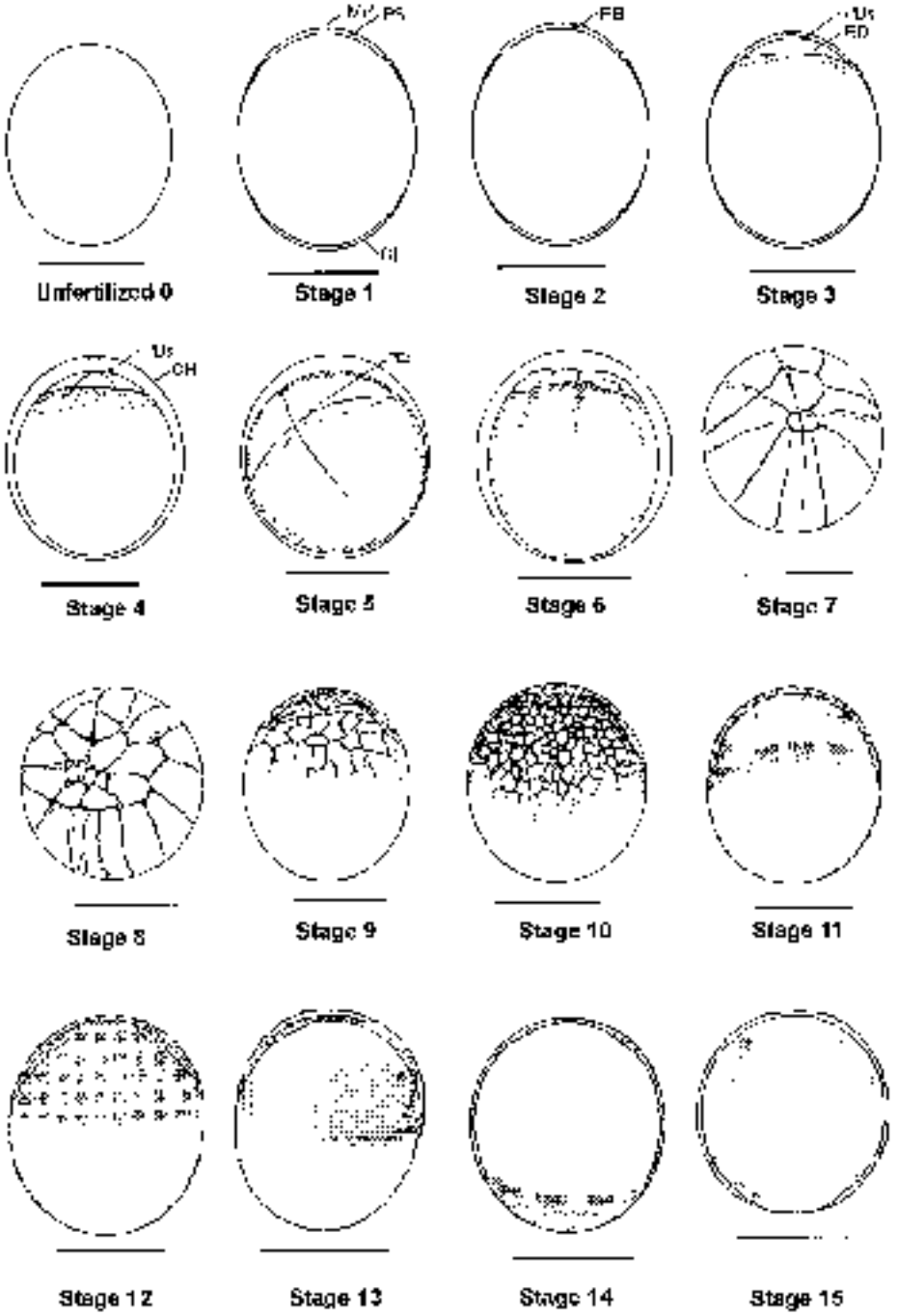

Fig. 1: Embryonic development of *Illex argentinus* from unfertilized egg to Stage 15. The chorion is omitted after Stage 6. Scale bar 0.5 mm. BD, blastodisc; CH, chorion; MP, micropyle; PB (PBs), first (second) polar bodies; PS, perivitelline space

petri dishes with fertilized eggs were put into incubators within five minutes of the fertilization procedure. The incubators were maintained at temperatures of 8.5, 11.4, 13.0, 15.0, 17.3, 20.1 and 23.2°C, and embryonic development was observed up to hatching at each temperature. A few embryos of uniform age were selected carefully for the observations, and representative embryos were drawn by hand and photographed. Detailed drawings were also made on a personal computer from pictures acquired with an image scanner from original photographs taken under a Nikon stereomicroscope.

The system of embryonic stages proposed by Watanabe *et al*. (1996) for *Todarodes pacificus* was followed to describe the developmental stages of *I. argentinus*. The criteria described by Arnold (1965) for *Loligo* and those of Naef (1921–1923) and O'Dor *et al*. (1982) for *Illex* were also considered. Roman numbers in parenthesis in the descriptions herein indicate the stages of Naef (1921–1923) and O'Dor *et al*. (1982). The long and short axes of eggs and chorions, and the dorsal mantle lengths (*ML*) of embryos and hatchlings were measured to the nearest 0.02 mm, using a stereomicroscope equipped with an ocular micrometer.

Hatchlings incubated at 20.1°C were measured and preserved in 90% alcohol or frozen for statolith observation. Statoliths were extracted with fine dissecting needles, carefully rinsed with distilled water, dried and covered with a small drop of the mounting medium ProTexx.

A video-image-analysis system (RATOC otolith daily ring measurement system), consisting of a high-resolution and -sensitivity monochrome CCD camera (SONY XC-77) mounted on an Olympus microscope (BX50) was used for statolith measurement. The microscope was connected to a high-resolution colour monitor (SONY PVM-2054Q) with a frame-grabber (Avio EXCEL-II), a Mitsubishi video printer installed in a NEC personal computer and a magnetic optical drive. The maximum statolith radius (*MSR*, the length from the focus to the widest part of the lateral margin, Nakamura 1987, Macy 1995) and the maximum statolith diameter were measured to the nearest 0.1 μm. Edge-enhancement-filtered images of statoliths were stored in the system as archival records. The terminology proposed for statoliths by Lipiński *et al*. (1991) was used.

ATLAS OF DEVELOPMENTAL STAGES

A total of 30 embryonic stages was defined from unfertilized ovum (Stage 0) to hatching (Stage 30). Unfertilized ova removed from the oviduct were oval, and fertilized ova maintained this shape until the first cleavage. During embryonic development, there were two phases of chorion expansion, the first (Fig. 1) about 20 minutes after fertilization at 23.2°C, when a perivitelline space appeared at the animal and vegetal poles. The second chorion expansion began after the blastoderm period (Stages 16 – 17) and continued through Stage 28, when the chorion diameter attained more than 2.5 mm.

Embryos developed and hatched at all five experimental temperatures between 13.0 and 23.2°C. At 8.5 and 11.4°C, the embryos stopped development at Stages 11 and 17 respectively. Hatching occurred 130–400 h after fertilization, depending on temperature, in the least disturbed eggs. The *ML* of embryos before hatching (Stage 28) was 1.4 mm at 23.2°C.

Fertilization, meiosis and cleavage (Fig. 1)

Stage 0 – Unfertilized ova are oval. Long axes range between 0.92 and 1.18 mm (mean 1.02 mm) and the short axes between 0.70 and 0.96 mm (mean 0.81 mm).

Stage 1, 20 minutes after fertilization at 23.2°C – Perivitelline space begins to develop at the animal and vegetal poles. Micropyle is visible at the animal pole.

Stage 2, 30 minutes at 23.2°C – First maturation division. First polar body appears near the animal pole.

Stage 3, 1.5 h at 23.2°C – Second maturation division. Second polar body appears beside the first polar body. The blastodisc, an area more transparent than the ooplasmic area, appears at the animal pole. Chorion expands at both animal and vegetal poles.

*Stage 4***,** 2.6 h at 23.2°C – First cleavage. A furrow occurs at the centre of the blastodisc running beneath the polar bodies and extending towards the equator of the egg (2 cells).

Stage 5, 3.6 h at 23.2°C – Second cleavage. The second cleavage furrow occurs across the first one at a right angle some distance from the polar bodies, and divides the first two cells into four.

*Stage 6***,** 4.3 h at 23.2°C – Third cleavage. The division is unequal, but the furrows are symmetrical in the right and left halves (8 cells).

*Stage 7***,** 5.1 h at 23.2°C – Fourth cleavage. It is

roughly parallel to the second furrow (16 cells, four form the first central blastomeres).

Stage 8, 6 h at 23.2°C – Fifth cleavage. Cleavage planes are largely radial (32 cells).

Stage 9, 6.7 h at 20.1°C – Sixth cleavage. The cells (about 64) divide asynchronously.

Stage 10 (Stage I of Naef 1921–1923), 12.0 h at 17.3°C – Cleavage continues asynchronously. A group of very small cells remains recognizable in the centre of the blastoderm. The blastomeres remain in a monolayer.

Segregation of the germ layers and growth of the blastoderm (Fig. 1)

Stage 11 (Stage III), 17 h at 17.3°C – A ring of cells has formed around the yolk mass below the margin of the blastoderm. The monolayer of blastomeres can be recognized because the adjacent cells cover a peripheral ring of two rows of blastomeres. Cell size becomes smaller and almost uniform.

Stage 12 (Stage V), 30 h at 17.3°C – The papilla-like yolk mass apex resembles a truncated cone in the animal pole, and the blastoderm covers half of the egg. The epibolic process continues, and the outer monolayer grows over and beyond the peripheral ring, which forms an inner layer. The inner layer spreads towards the animal pole below the outer layer. The edge of the blastoderm expands towards the vegetal pole.

Stage 13, 44 h at 17.3°C – The blastoderm covers about two-thirds of the egg. The papilla-like yolk apex gradually becomes smaller when the inner germ layer reaches a position near the animal pole.

Stage 14, 53 h at 17.3°C – The blastoderm covers more than three-quarters of the egg. The edge of the spreading blastoderm forms a ring around the vegetal pole. The papilla-like yolk apex almost disappears.

Stage 15, 60 h at 17.3°C – The edge of the spreading blastoderm almost reaches the vegetal pole. The papilla-like yolk apex disappears.

Organogenesis and hatching (Figs 2, 3)

Stage 16 (Stage VII), 112 h at 15.0°C – The edge of the spreading blastoderm reaches over the vegetal pole. Eye and mouth primordia are evident as thickenings in the blastoderm.

Stage 17 (Stage VIII), 120 h at 15°C – Elevation of mantle and invagination of shell gland on the mantle begin at the posterior end of the embryo. Primordia of eyes are visible as disc-like elevations (Fig. 4a). Invagination of mouth is visible in the dorsal view between the eyes. Longitudinal expansion of the embryo and the chorion begins.

Stage 18 (Stage IX), 147 h at 15.0°C – Mantle development begins and the shell gland is nearly closed. Yellow pigmentation of eyes begins. Elevation of tentacles and Arms II is visible on the ventral side and on the anterior margin of the embryo respectively. The funnel tube elevates slightly in the ventral middle of the embryo. Embryo revolves slowly in the perivitelline space. Chorion expansion continues.

Stage 19 (Stage X), 150 h at 15.0°C – Formation of mantle margin and mantle cavity begins. The funnel folds are clearly visible. Primordia of statocysts appear as small vesicles at the anterior part of the distal edges of the funnel folds (Fig. 4b). Chorion expansion continues. A row of faint chromatophores is visible on the dorsal mantle margin.

Stage 20 (Stage XI), 165 h at 15.0°C – The mantle margin grows anteriorly and the mantle cavity spreads into the dorsum. Red pigmentation in retina. Hoyle's organ is first visible on the dorsal mantle. Funnel folds develop as a belt from ventral to dorsal. Two rows of chromatophores are visible on the ventral and anterior mantle. A group of chromatophores appears in the cephalic region on both ventral and dorsal sides.

Stage 21, 172 h at 15.0°C – Mantle length is one-third of the total length of the embryo. Primordia of Arms I are visible in ventral view. Eye stalks increase in height.

Stage 22 (Stage XII), 185 h at 15.0°C – Funnel folds fuse and form a triangular shape with a slit at the midline. Mantle length is about 40% of the embryo length. Mantle does not cover the posterior margin of the funnel. First sucker primordia appear on the tentacle tips.

Stage 23 (Stage XIII), 195 h at 15.0°C – Mantle reaches the posterior margin of the funnel, and mantle length is one-half of the embryo length. Fin primordia appear on the apex of the mantle. Funnel folds form a complete tube. Three sucker primordia on the tentacle tips.

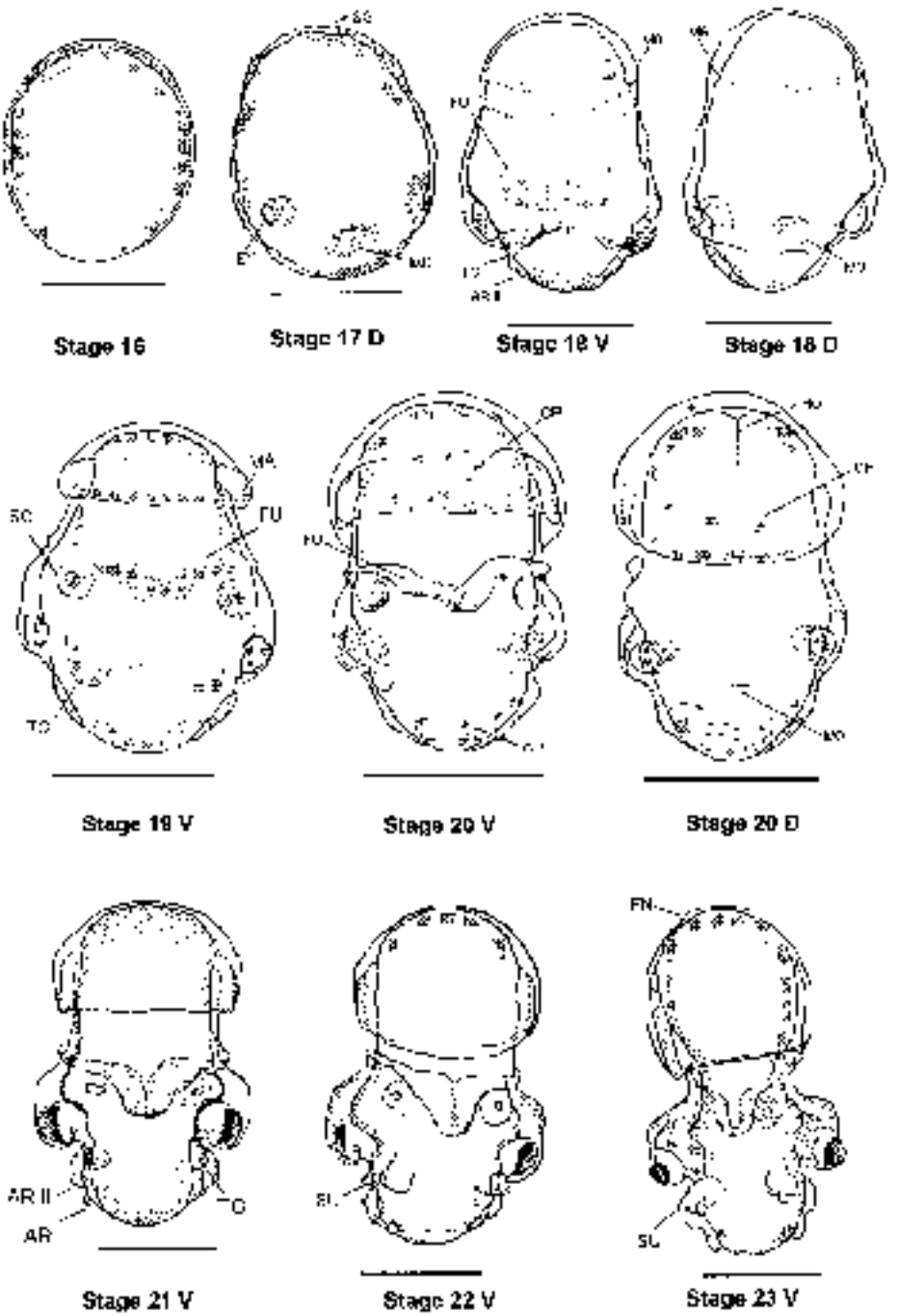

Fig. 2: Embryonic development of *Illex argentinus* from Stages 16 to 23. Chorion is omitted. D or V with stage number indicates dorsal or ventral view respectively. Scale bar 0.5 mm. AR, arm; CP, chromatophore; EY, eye; FN, fin; FU, funnel; HO, Hoyle's organ; MA, mantle; MO, mouth; SC, statocyst; SG, shell gland; SU, sucker; TC, tentacle

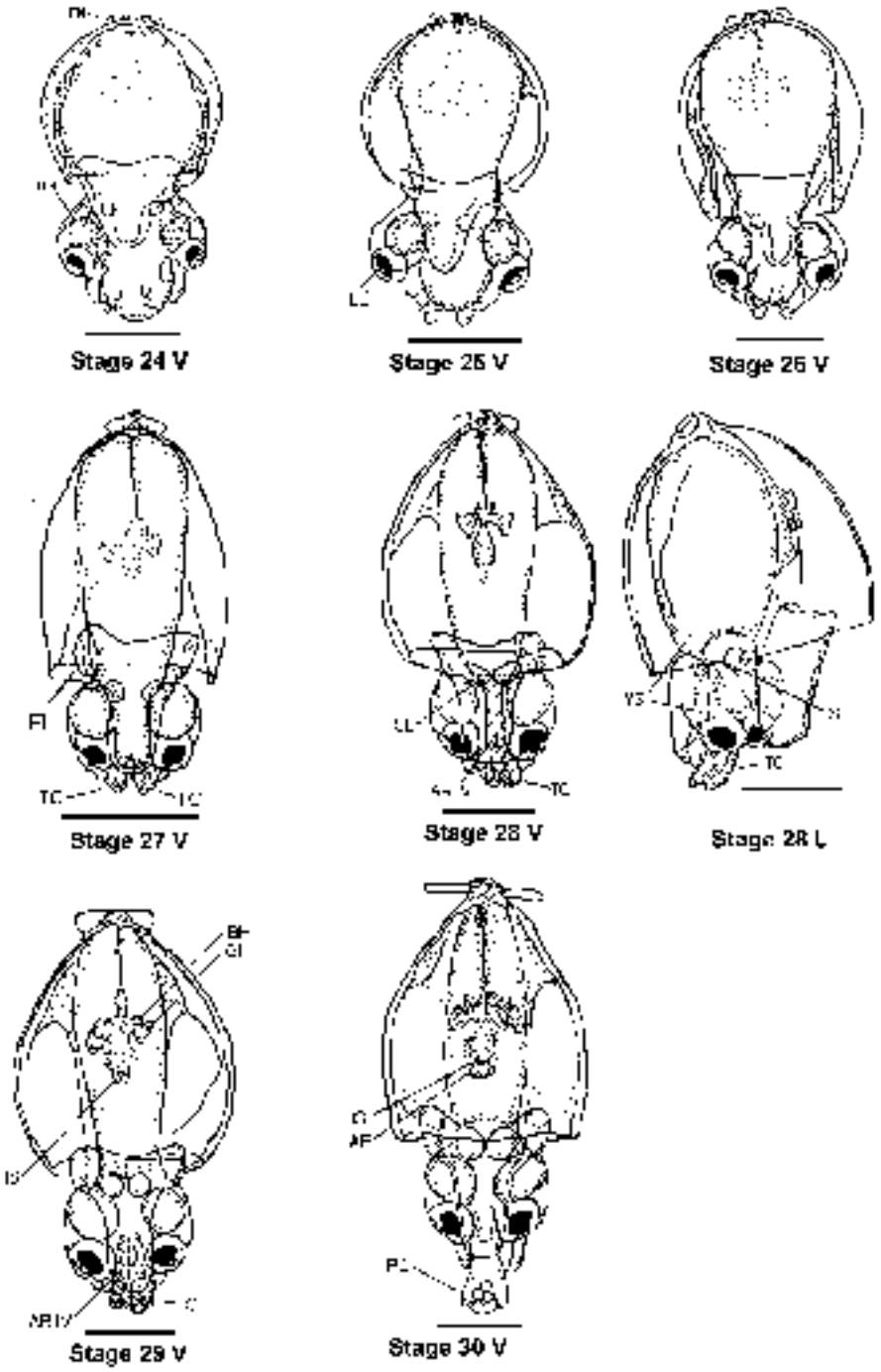

Fig. 3: Embryonic development of *Illex argentinus* from Stages 24 to 30. Chorion is omitted. L or V with stage number indicates lateral or ventral view respectively. Scale bar 0.5 mm. AR, arm; AP, anal papilla; BH, branchial heart; FL, funnel-locking apparatus; FN, fin; GI, gill; IS, ink sac; LE, lens; OG, optic ganglion; PC, proboscis; SL, statolith; TC, tentacle; YS, yolk sac

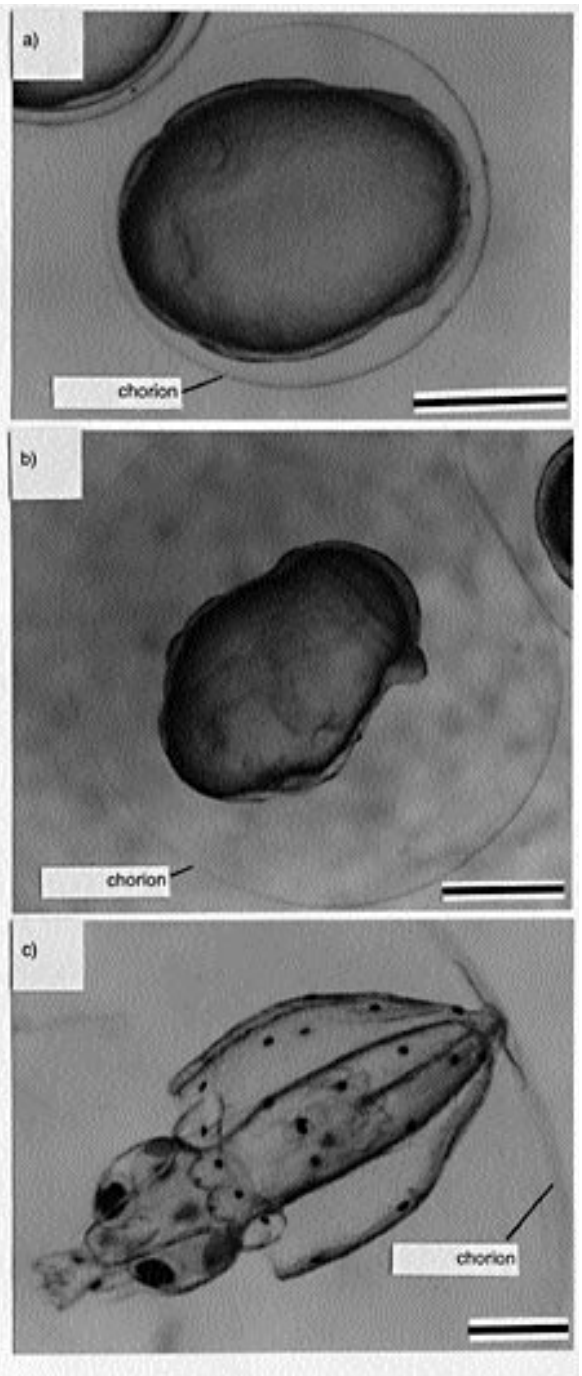

Fig. 4: *Illex argentinus* embryos from artificial fertilization. (a) Stage 17, (b) Stage 19, showing expanded chorion, (c) Stage 30, just before hatching at 1.58 mm *ML*. Scale bar 0.5 mm

Stage 24 (Stage XIV), 214 h at 15.0°C – Mantle extends over one-half of the total embryo length and covers the posterior margin of the funnel. The mantle occasionally contracts. Primordia of ventral organs are faintly visible. Four sucker primordia on the tentacle tips and one sucker primordium on Arms I and II. Optic ganglia appear on the posterior side of the eye vesicles.

Stage 25 (Stages XIV–XV), 220 h at 15.0°C – Internal yolk sac begins bifurcating at the posterior apex, but the split is not visible externally. Lens primordia are first visible. Primordia of ventral organs, such as the heart-gill complex and the branchial heart, become clear and are trifoliate in shape.

Stage 26 (Stages XV–XVI), 230 h at 15.0°C – The split in the posterior apex of the internal yolk sac is evident. The bases of the two tentacles come together in the anterior apex of the external yolk sac, but are not completely fused. Embryo glides backwards slowly by ciliary action along the expanded chorion.

Stage 27 (Stages XVI-XVII), 237 h at 15.0°C – Internal yolk sac bifurcates towards the base of the ventral organs. Tentacles are nearly fused. Funnel-locking apparatus is forming on the posterior edges of the funnel.

Stage 28 (Stage XVII), 245 h at 15.0°C – Primordia of Arms IV are first visible as two faint swellings on the bases of the fused tentacles between both eyes in ventral view. Statoliths are visible in the anterior parts of the statocysts. The heart-gill complex is clearly visible, and the branchial hearts occasionally pulsate. The yolk sac in the cephalic region contracts. Hatching may occur as a result of external stimulation.

Stage 29 (Stage XVIII+), 305 h at 15.0°C – Ink sac is first visible as a small vesicle on the primordium of the rectum, but no ink is present. The fused tentacles begin to elongate as a proboscis. Faint swellings of anal papillae appear on the anterior margin of the primordium of the rectum. Primordia of gills and branchial hearts are evident. The digestive gland is visible as a faint swelling under the primordium of the rectum. The yolk sac in the cephalic region almost disappears, but it is still visible as a duct.

Stage 30 (Stage XX), 340 h at 15.0°C – Hatching occurs in eggs least disturbed during incubation. Ink sac fills with ink, which the hatchling ejects when stimulated. The buccal mass and the fins are functional. Fin width nearly equals head width (Fig. 4c). The proboscis is extensible.

HATCHING PARALARVAE

Paralarvae hatched at Stage 30 were principally characterized by the development of functional fins and an ink sac. The mean mantle length of a hatchling incubated at 20.1C was 1.59 mm (*SD* 0.04 mm, $n = 44$). They were able to swim off the bottom of a small container. When stimulated externally, they ejected ink. They survived 7 – 10 days at 17.3°C without feeding. Hatching from disturbed eggs may occur at Stage 28. It then took between about 2 and 4.5 days at 23.2 and 13.0°C respectively to reach Stage 30.

Statoliths were extracted from Stage 30 hatchlings incubated at 20.1°C (Fig. 5a, b). The mean maximum statolith radius *MSR* was 20.1 µm (*SD* 1.8 µm, $n = 23$) and the mean maximum statolith length 32.1 µm (*SD* 2.3 µm, $n = 23$). A smaller statolith extracted from a premature hatchling at Stage 28 had a *MSR* of 10.2 µm and a statolith diameter of 23.3 µm, with a focus in its centre (Fig. 5c, d). This statolith had no ring-like increments, so its outer edge appears to correspond to the nucleus. In statoliths from Stage 30 hatchlings, however, 4 – 6 rings were observed (Fig. 5b). As it took about 2 days between Stages 28 and 30 at 20.1°C, these rings would appear to be subdaily increments.

DISCUSSION

The present study describes 30 developmental stages for *I. argentinu*s embryos fertilized *in vitro*. The stages are based mainly on morphological features and can be distinguished clearly under a stereomicroscope. Some behavioural features were also included as criteria for stage determination. Since Naef (1921–1923) described embryonic development of an ommastrephid later identified as *I. coindetii* based on chronological age, several authors have adopted his developmental stages for *Illex* species (Boletzky *et al*. 1973, O'Dor *et al*. 1982). The embryonic stages proposed for *I. coindetii* by Naef (1921–1923), however, lacked odd-numbered stages and stages before VIII. O'Dor *et al*. (1982) presented embryonic stages for *I. illecebrosus,* adding odd numbers to Naef's stages. However, they did not describe all stages. Recently, Watanabe *et al*. (1996) described detailed developmental stages for *Todarodes pacificus* from fertilized egg to 7- day-old paralarva (Stage 34), based on the morphological features proposed by Arnold (1965) and with histological confirmation.

The current observations on the embryonic development of *I. argentinus* correspond closely with those proposed for *I. coindetii* by Naef (1921–1923) and for *I. illecebrosus* by O'Dor *et al*. (1982), in spite of the different criteria for developmental stages used in the earlier studies. The present observations also coincide with those proposed by Watanabe *et al*. (1996) for *T. pacificus* from fertilization to organogenesis, but there are several differences in development between the two species after Stage 19. Two morphological events apparently take place earlier in *I. argentinus* than in *T. pacificus*. Whereas the statocysts of *T. pacificus* appear at Stage 21 as invaginations, the invaginations appeared at Stage 19 in *I. argentinus*. Statoliths appeared at Stage 28 in both species.

A significant difference between the two species is the appearance of fin primordia at Stage 28 in *T. pacificus*, but at Stage 23 in *I. argentinus*. The outer yolk sac in the cephalic region disappears during Stages 27 and 28 in *T. pacificus*, slightly earlier than in *I. argentinus* (Stages 28 and 29), *I. coindetii* and *I. illecebrosus*. These hatchlings had developed fins and functional ink sacs, similar to *I. illecebrosus* Stage XX hatchlings from naturally spawned eggs (O'Dor *et al.* 1982) and to *I. coindetii* hatchlings (Naef 1921–1923). Stage 30 is considered to be the *in vitro* hatching stage for *I. argentinus*.

Hatching size (1.59 mm *ML*) was larger than that described for the same species (0.9–1.2 mm) by Sakai and Brunetti (1997), for *I. illecebrosus* (1.1 mm, Durward *et al.* 1980) and *T. pacificus* (0.95 mm, Watanabe *et al*. 1996). The *I. argentinus* hatchlings observed by Sakai and Brunetti (1997) probably hatched prematurely, because they displayed characteristcs of Stage 28. Durward *et al*. (1980) and O'Dor *et al*. (1982) documented hatching 6–8 days (at 13°C) and 16 days (at 12–14°**C**) after spawning, respectively, in *I. illecebrosus*. Considering the current results, which agree with those of O'Dor *et al*. (1982), it may well be that the embryos observed by Durward *et al*. (1980) had hatched prematurely. Boletzky *et al*. (1973) observed embryonic development of *I. coindetii* spawned in a tank. They did not describe the size of normal hatchlings, but the mantle length of an embryo before hatching was 1.4 mm *ML*, the same size as *I. argentinus* before hatching in the present study.

Watanabe *et al*. (1996) noted the morphological differences in hatching stages among *Illex* spp. and *T. pacificus*, but they did not mention whether these differences could be attributable to differences between species or to environmental factors. Hatching stages seem to be different in the genera *Illex* and *Todarodes*. The morphological features of hatchlings suggest that species of *Illex* hatch at a more advanced embryonic stage than does *T. pacificus*. There are also apparent differences in egg size and fecundity between *I. argentinus* and *T. pacificus*. Egg axis lengths (1.02 × 0.81 mm in this study) and fecundity (about 15 000–

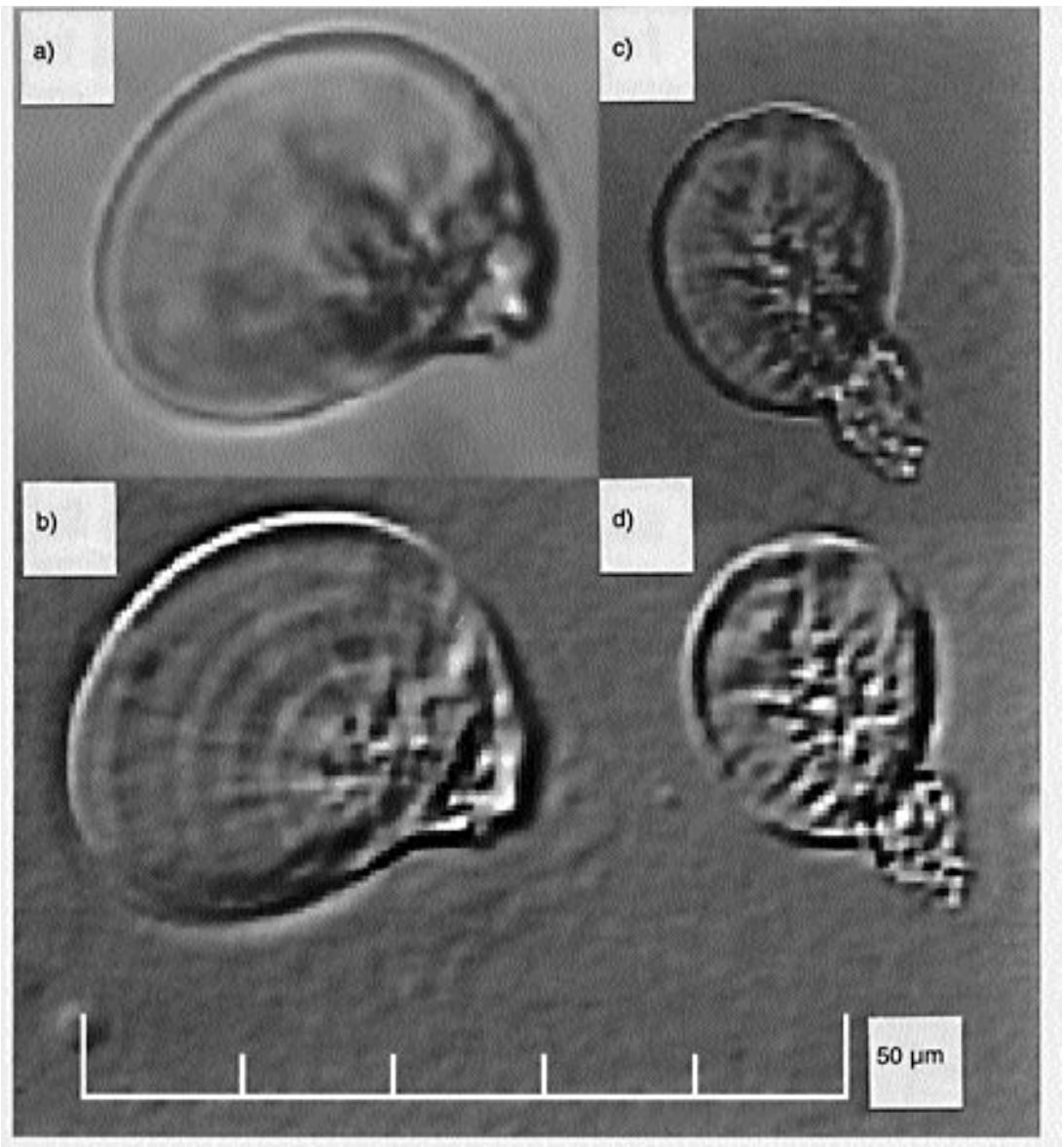

Fig. 5: Statoliths from laboratory-reared *Illex argentinus* hatchlings. (a) Raw image, statolith extracted from a Stage 30 hatchling of 1.54 mm *ML*; (b) edge-enhancement-filtered image applied to (a); (c) raw image, statolith extracted from a Stage 28 hatchling of 1.32 mm *ML*; (d) edge-enhancement-filtered image applied to same panel of (c)

140 000, Brunetti *et al*. 1991) of *I. argentinus* are somewhat different from the values documented for *T. pacificus* (0.83 and 0.70 mm, Watanabe *et al*. 1996; 304 000 – 470 000, Soeda 1956, Bower and Sakurai 1996). *I. argentinus* females produce larger eggs and are less fecund than *T. pacificus*. Furthermore, embryonic development takes twice as long in *I. argentinus* (340 h at 15.0°C) as in *T. pacificus* (168 h at 14.7°C, Sakurai *et al.* 1996). It is suggested that these differences in early life history are due to differ-

ences between species in such reproductive features as egg size, clutch size and early ontogeny.

Embryonic development of *I. argentinus* ceased before hatching at 8.5°C and 11.4°C. Many authors (Hamabe 1961a, b, Boletzky *et al*. 1973, O'Dor *et al*. 1982, Sakurai *et al*. 1996) have suggested minimum temperatures for normal embryonic development in ommastrephid squid. O'Dor *et al*. (1982) showed experimentally that *I. illecebrosus* eggs failed to develop at temperatures <12°C. Sakurai *et al*. (1996) concluded that the best survival rates (> 70%) for *T. pacificus* paralarvae were between 14.7 and 22.2°C, and suggested that females must spawn in waters warmer than 12.1°C. Brunetti (1990) suggested that *I. argentinus* egg masses spawned in summer lie in the upper water layers where temperatures exceed 13°C. Brunetti and Ivanovic (1992) reported that the paralarvae of winter-spawning *I. argentinus* are not found in water <14°C. Current observations suggest that the minimum temperature for normal development in *I. argentinus* lies between 11.4 and 13.0°C.

There are few studies on statoliths of ommastrephid hatchlings, which may in part be the result of difficulties in obtaining hatchlings *in vitro*. In the present study, 4–6 increments had formed in the statoliths extracted from Stage 30 hatchlings *in vitro*. The statolith size at Stage 28 was 23.3 µm, similar to that of 0-day-old *I. illecebrosus* hatchlings (Balch *et al*. 1988), whereas it was 32.1 µm at Stage 30, close to those of 3-day-old *I. illecebrosus* hatchlings (27.4 µm, Dawe *et al.* 1985; 42 µm, Balch *et al.* 1988). Statolith size at hatching for *I. argentinus* was larger than for *I. illecebrosus*. Statoliths at the normal hatching stage (Stage 30) already have several growth increments, which appear to form subdaily. Further studies on the increments of statoliths with both laboratory-reared and wild hatchlings may reveal the true statolith features in the early life stage of *Illex* species.

ACKNOWLEDGEMENTS

We thank the masters, officers and crew of INIDEP's R.V. *Capitan Oca Balda* for their cooperation, and the squid research staff of INIDEP for assistance. Thanks are also due to Dr S. Chikuni, Team Leader of the JICA (Japan International Cooperation Agency) project, for his continued encouragement. Finally we acknowledge the efforts of Dr J. R. Bower, Hokkaido University, Ms M. L. Ivanovic, INIDEP, Dr S. von Boletzky, Laboratoire Arago, France, and Dr J. A. A. Perez, Falculdade de Ciências do Mar, Brazil, in providing valuable comments on earlier drafts of the manuscript. The study was supported by a cooperative project of JICA and INIDEP (Assessment and Monitoring of Fisheries Resources).

LITERATURE CITED

ARNOLD, J. M. 1965 — Normal embryonic stages of the squid *Loligo pealii* (LeSueur). *Biol. Bull. mar. biol. Lab., Woods Hole* **128**(1): 24–32.

BALCH, N., SIROIS, A. and G. V. HURLEY 1988 — Growth increments in statoliths from paralarvae of the ommastrephid squid *Illex* (Cephalopoda: Teuthoidae). *Malacologia* **29**(1): 103–112.

BOLETZKY, S. von, ROWE, L. and L. AROLES 1973 — Spawning and development of the eggs, in the laboratory, of *Illex coindetii* (Mollusca: Cephalopoda). *Veliger* **15**(3): 257–258.

BOWER, J. R. and Y. SAKURAI 1996 — Laboratory observations on *Todarodes pacificus* (Cephalopoda: Ommastrephidae) egg masses. *Am. malacol. Bull.* **13**(1–2): 65–71.

BRUNETTI, N. E. 1990 — Description of rhynchoteuthion larvae of *Illex argentinus* from the summer spawning subpopulation. *J. Plankt. Res*. **12**(5): 1045–1057.

BRUNETTI, N. E., IVANOVIC, M. L., LOUGE, E. and H. E. CHRISTIANSEN 1991 — Estudio de la biología reproductiva y de la fecundidad en dos subpoblaciones del calamar (*Illex argentinus*). *Frente mar., Sec. A* **8**: 73–84.

BRUNETTI, N. E. and M. L. IVANOVIC 1992 — Distribution and abundance of early life stages of squid (*Illex argentinus*) in the south-west Atlantic. *ICES J. mar. Sci*. **49**: 175–183.

DAWE, E. G., O'DOR, R. K., ODENSE, P. H. and G. V. HURLEY 1985 — Validation and application of an ageing technique for short-finned squid (*Illex illecebrosus*). *J. NW. Atl. Fish. Sci.* **6**: 107–116.

DURWARD, R. D., VESSEY, E., O'DOR, R. K. and T. AMARATUNGA 1980 — Reproduction in the squid, *Illex illecebrosus*: first observations in captivity and implications for the life cycle. *Sel. Pap. int. Commn NW. Atl. Fish.* **6**: 7–13.

HAIMOVICI, M., VIDAL, E. A. G. and J. A. A. PEREZ 1995 — Larvae of *Illex argentinus* from five surveys on the continental shelf of southern Brazil. *ICES mar. Sci. Symp*. **199**: 414–424.

HAMABE, M. 1961a — Experimental studies on breeding habit and development of the squid, *Ommastrephes sloani pacificus* Steenstrup. 2. Spawning behavior. *Zool. Mag.* **70**: 385–394 (in Japanese with English abstract).

HAMABE, M. 1961b — Experimental studies on breeding habit and development of the squid, *Ommastrephes sloani pacificus* Steenstrup. 3. Early embryonic development and morphological features of the larvae immediately after hatching. *Zool. Mag.* **70**: 408–420 (in Japanese with English abstract).

IKEDA, Y., SAKURAI, Y. and K. SHIMAZAKI 1993 — Fertilizing capacity of squid (*Todarodes pacificus*) spermatozoa collected from various sperm storage sites, with special reference to the role of gelatinous substance from oviducal gland in fertilization and embryonic development. *Invert. Reprodn Dev.* **23**(1): 39–44.

LIPIŃSKI, M. [R], DAWE, E. [G] and Y. NATSUKARI 1991 — Practical procedures of squid ageing using statoliths. A laboratory manual. Introduction. In *Squid Age Determination using Statoliths. Proceedings of an International Workshop, Mazara del Vallo, Italy October 1989.* Jereb, P., Ragonese, S. and S. von Boletzky (Eds). *Spec. Publ. NTR-ITPP* **1**: 77–81.

MACY, W. K. 1995 — The application of digital image processing to the aging of long-finned squid, *Loligo pealei*, using

the statolith. In *Recent Developments in Fish Otolith Research.* Secor, D. H., Dean, J. M. and S. E. Campana (Eds). Columbia, South Carolina; University of South Carolina Press: 283–302.

NAEF, A. 1921-1923 — *Cephalopoda. Fauna e Flora del Golfo di Napoli, Monograph* **35**: 917 pp. (translated from German by the Israel Program for Scientific Translations, Jerusalem,1972).

NAKAMURA, Y. 1987 — Observation of statoliths of juvenile *Todarodes pacificus* caught by coastal set net in the Iwate prefecture. Report of annual meeting on resource and fisheries of squids. *Jap. Sea Reg. Res. Lab*. **9**: 73–76 (in Japanese).

O'DOR, R. K., BALCH, N., FOY, E. A., HIRTLE, R. W. M., JOHNSTON, D. A. and T. AMARATUNGA 1982 — Embryonic development of the squid, *Illex illecebrosus*, and effect of temperature on developmental rates. *J. NW. Atl. Fish. Sci*. **3**(1): 41–45.

O'DOR, R. K., DURWARD, R. D. and N. BALCH 1977 — Maintenance and maturation of squid (*Illex illecebrosus*) in a 15 meter circular pool. *Biol. Bull. mar. biol. Lab., Woods Hole* **153**(2): 322–335.

RODHOUSE, P. G., BARTON, J., HATFIELD, E. M. C. and C. SYMON 1995 — *Illex argentinus*: life cycle, population structure, and fishery. *ICES mar. Sci. Symp*. **199**: 425–432.

SAKAI, M. and N. E. BRUNETTI 1997 — Preliminary experiments on artificial insemination of the Argentine shortfin squid *Illex argentinus*. *Fish. Sci.* **63**(5): 664–667.

SAKURAI, Y., BOWER, J. R., NAKAMURA, Y., YAMAMOTO, S. and K. WATANABE 1996 — Effect of temperature on development and survival of *Todarodes pacificus* embryos and paralarvae. *Am. malacol. Bull.* **13**(1–2): 89–95.

SAKURAI, Y., YOUNG, R. E., HIROTA, J., MANGOLD, K., VECCHIONE, M., CLARKE, M. R. and J. R. BOWER 1995 — Artificial fertilization and development through hatching in the oceanic squids *Ommastrephes bartramii* and *Sthenoteuthis oualaniensis* (Cephalopoda: Ommastrephidae). *Veliger* **38**(3): 185–191.

SOEDA, J. 1956 — Studies on the ecology and the breeding habits of the squid, *Ommastrephes sloani pacificus* (Steenstrup). *Bull. Hokkaido reg. Fish. Res. Lab*. **14**: 1–24 + 4 Plates (in Japanese, with English abstract).

WATANABE, K., SAKURAI, Y., SEGAWA, S. and T. OKUTANI 1996 — Development of the ommastrephid squid *Todarodes pacificus*, from fertilized egg to rhynchoteuthion paralarva. *Am. malacol. Bull.* **13**(1–2): 73–88.